

Parametrically Excited Non-Linear Traveling Beams with and without External Forcing

G. CHAKRABORTY and A. K. MALLIK*

Department of Mechanical Engineering, Indian Institute of Technology, Kanpur, U.P. – 208016, India

(Received: 30 January 1998; accepted: 17 August 1998)

Abstract. The effects of parametric excitation on a traveling beam, both with and without an external harmonic excitation, have been studied including the non-linear terms. Non-linear, complex normal modes have been used for the response analysis. Detailed numerical results are presented to show the effects of non-linearity on the stability of the parametrically excited system. In the presence of both parametric and external harmonic excitations, the response characteristics are found to be similar to that of a Duffing oscillator. The results are sensitive to the relative strengths of and the phase difference between the two forms of excitations.

Keywords: Parametric excitation, non-linear complex normal mode, stability, jump phenomena.

1. Introduction

Band saws, magnetic and paper tapes, traveling threadlines are some examples of traveling continuous systems. Such systems are modeled as axially moving strings or beams with simply supported end conditions [1]. The axial movement of the slender member is often sustained by rotating pulleys. These pulleys are either rigidly or flexibly mounted upon the foundation. Beyond a critical speed of the axial movement, buckling or divergence instability occurs. Normally, a finite pulley-support compliance in the axial direction provides a stabilizing effect. For a band saw, however, sometimes the presence of unbalance in the flexibly mounted pulleys may cause parametric excitation, which in turn causes instability in a statically stable system. For a belt driven by pulleys, the parametric excitation is primarily caused by the belt defects [2] and the torque pulses generated in the driving mechanisms.

A linear analysis has been widely applied [3, 4] to determine the onset of parametric instability in a traveling beam. The primary parametric instability and the fundamental summation resonance have been given special attention. The mode shapes of a stationary beam are used to obtain a set of coupled, linear differential equations having periodic coefficients.

Non-linearities have long been recognized to play a significant role in the parametrically excited Duffing oscillator [5]. The exponential growth of the amplitude, predicted by neglecting the non-linear term, is limited by the non-linearity resulting in a steady-state solution with finite amplitude. These solutions have been referred to as 'limit cycles' in the literature. The existence of limit cycles in a traveling string has been reported recently [6]. In this reference, the equation of motion has been discretized to a set of coupled, non-linear ordinary differential equations with time-varying coefficients. The complex linear eigenfunctions were used to this end.

* Author for correspondence.

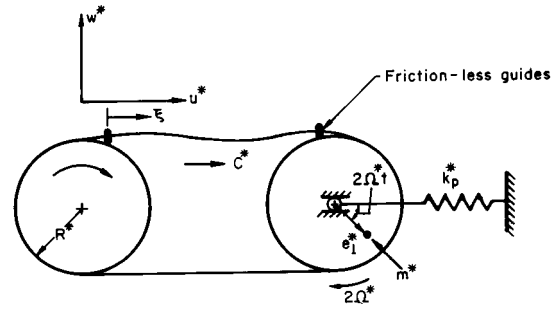


Figure 1. Schematic diagram of a traveling beam having parametric excitation.

The effects of both external and parametric excitations on a Duffing oscillator have also been studied [7, 8]. The response is normally aperiodic. But if the frequencies of the two forms of excitation are synchronized, a steady-state harmonic solution is resulted. Superharmonics and subharmonics may also result if some special relationships exist between the frequencies of the two forms of excitation.

For non-linear, multi-degrees-of-freedom and continuous systems having linear boundary conditions, the concept of non-linear normal modes has been used fruitfully to obtain the near-resonance response under a harmonic excitation [9]. Since the stationary normal modes do not exist for a traveling continuous system, complex non-stationary, non-linear normal modes have also been derived [10]. These modes have then been used to compute the near-resonance response of a harmonically excited traveling beam.

In the present work, the primary resonance (under parametric excitation) of a traveling beam has been studied including the non-linear terms. To this end, again the concept of non-linear, complex normal mode has been used. The limit cycle amplitudes and their stabilities have been given special attention. The excitation of other linear modes besides the primarily excited one is clearly brought out. Numerical results are also presented to show the effects of different system parameters (like band speed, pulley compliance) on the limit cycle amplitudes. The effects of inclusion of the non-linear terms are seen to be very similar to those exhibited by a Duffing oscillator.

The non-linear, complex normal modes are then used to obtain the steady-state harmonic response of a traveling beam when both forms of excitation, namely, parametric and external harmonic, are present. The results are obtained by numerically solving a fifth order polynomial equation. Numerical computations show that the phase difference between the external forcing and the parametric excitation affects the overall response amplitude. The response characteristics are also governed by the relative strengths of the two forms of excitation.

2. Equations of Motion

Let us consider a traveling slender beam, driven by a pulley as shown in Figure 1. The finite pulley compliance is modeled by a linear spring. Under the usual assumption $u^* = O(w^*)^2$, the equations of motion for undamped planar vibration including the non-linear terms are [11]:

$$\rho A \left[\frac{\partial^2 u^*}{\partial t^2} + 2c^* \frac{\partial^2 u^*}{\partial \xi \partial t} + c^{*2} \frac{\partial^2 u^*}{\partial \xi^2} \right] - EA \frac{\partial^2 u^*}{\partial \xi^2} = (EA - T^*) \frac{\partial w^*}{\partial \xi} \frac{\partial^2 w^*}{\partial \xi^2} \quad (1)$$

and

$$\begin{aligned} \rho A \left[\frac{\partial^2 w^*}{\partial t^2} + 2c^* \frac{\partial^2 w^*}{\partial \xi \partial t} + c^{*2} \frac{\partial^2 w^*}{\partial \xi^2} \right] - T^* \frac{\partial^2 w^*}{\partial \xi^2} + EI_z \frac{\partial^4 w^*}{\partial \xi^4} \\ = (EA - T^*) \frac{\partial}{\partial \xi} \left[\frac{\partial u^*}{\partial \xi} \frac{\partial w^*}{\partial \xi} + \frac{1}{2} \left(\frac{\partial w^*}{\partial \xi} \right)^3 \right]. \end{aligned} \quad (2)$$

The symbols used in Equations (1) and (2) are explained in Appendix I. The equilibrium tension T^* and the initial tension T_0^* are related as [12]

$$T^* = T_0^* + \eta \rho A c^{*2}, \quad (3)$$

where

$$\eta = 1 / \left(1 + \frac{k_p^* l}{2AE} \right); \quad 0 \leq \eta \leq 1. \quad (4)$$

Neglecting the curvature beyond the frictionless guides, the non-linear boundary conditions can be written as follows:

$$w^*(0, t) = w^*(l, t) = 0, \quad (5)$$

$$\frac{\partial^2 w^*(0, t)}{\partial \xi^2} = \frac{\partial^2 w^*(l, t)}{\partial \xi^2} = 0, \quad (6)$$

$$u^*(0, t) = 0, \quad (7)$$

and

$$\left[\frac{\partial u^*}{\partial \xi} + \frac{1}{2} \left(\frac{\partial w^*}{\partial \xi} \right)^2 \right]_{\xi=l} EA + \frac{k_p^*}{2} u^*(l, t) = 2m^* \Omega^{*2} e_1^* \cos 2\Omega^* t. \quad (8)$$

Equation (8) is obtained by balancing the horizontal forces at the elastically mounted pulley.

Attention may be drawn to the fact that in the absence of any frictionless guide, the dynamics of the two spans of the band/wheel system are coupled [13, 14] owing to the finite band curvature at the band-wheel interface. The coupling becomes less significant with increasing wheel radius and/or static tension and also with decreasing flexural rigidity of the band. It is well known [15-17] that the static deformation of the band increases monotonically with the axial speed. However, this deformation is reduced by incorporating the frictionless guides. Consequently, the simply-supported boundary conditions for the transverse vibration can now be conveniently used.

The following non-dimensional parameters (also see Appendix I) are used:

$$\begin{aligned} u = u^*/l, \quad w = w^*/(l\gamma^2), \quad x = \xi/l, \quad \tau = \left(\frac{E}{\rho} \right)^{1/2} \gamma t/l, \quad c = c^* \left(\frac{E}{\rho} \right)^{-1/2} \frac{1}{\gamma}, \\ k_p = k_p^* l / (2EA), \quad \Omega^* t = \Omega \tau, \quad 2m^* = m / (\rho Al), \quad e_1 = e_1^* / (\gamma^2 l), \\ T_0 = T_0^* / (EA\gamma^2), \quad R = R^* / l, \quad \gamma = r/l. \end{aligned} \quad (9)$$

It may be pointed out that the non-dimensionalized parameters u and w are now related as $u = O(\gamma^4 w^2)$.

Using Equation (3) and the non-dimensional parameters, the equations of motion and the boundary conditions are rewritten as

$$\left[\frac{\partial^2 u}{\partial \tau^2} + 2c \frac{\partial^2 u}{\partial x \partial \tau} + c^2 \frac{\partial^2 u}{\partial x^2} \right] - \frac{1}{\gamma^2} \frac{\partial^2 u}{\partial x^2} = \gamma^2 (1 - \gamma^2 T_0 - \gamma^2 c^2 \eta) \frac{\partial w}{\partial x} \frac{\partial^2 w}{\partial x^2}, \quad (10)$$

$$\begin{aligned} & \frac{\partial^2 w}{\partial \tau^2} + 2c \frac{\partial^2 w}{\partial x \partial \tau} + (kc^2 - T_0) \frac{\partial^2 w}{\partial x^2} + \frac{\partial^4 w}{\partial x^4} \\ & = (1 - \gamma^2 T_0 - \gamma^2 c^2 \eta) \frac{\partial}{\partial \xi} \left[\frac{1}{\gamma^2} \frac{\partial u}{\partial x} \frac{\partial w}{\partial x} + \frac{\gamma^2}{2} \left(\frac{\partial w}{\partial x} \right)^3 \right], \end{aligned} \quad (11)$$

$$w(0, \tau) = w(1, \tau) = 0, \quad (12)$$

$$\frac{\partial^2 w(0, \tau)}{\partial x^2} = \frac{\partial^2 w(1, \tau)}{\partial x^2} = 0, \quad (13)$$

$$u(0, \tau) = 0, \quad (14)$$

$$\left[\frac{\partial u}{\partial x} + \frac{\gamma^4}{2} \left(\frac{\partial w}{\partial x} \right)^2 \right]_{x=1} + \frac{k_p}{2} u(1, \tau) = \gamma^4 m \Omega^2 e_1 \cos 2\Omega \tau, \quad (15)$$

where $k = 1 - \eta$. It is easy to see from Equation (4) that $k = 1$ implies a rigidly mounted pulley, i.e., $k_p^* \rightarrow \infty$. Moreover, from Equations (4) and (9) one notes that k_p and k are related as

$$k_p / (1 + k_p) = k \quad \text{and} \quad 1 / (1 + k_p) = 1 - k. \quad (16)$$

Since $\gamma \ll 1$ implies that the speed of the longitudinal waves is much higher than that of the transverse waves, one can neglect the longitudinal inertia term in Equation (10) and gets (neglecting terms of order higher than γ^2)

$$-\frac{1}{\gamma^2} \frac{\partial^2 u}{\partial x^2} = \gamma^2 \frac{\partial w}{\partial x} \frac{\partial^2 w}{\partial x^2}, \quad (17)$$

which, when integrated twice, results in

$$u(x, \tau) = -\frac{\gamma^4}{2} \int_0^x \left(\frac{\partial w}{\partial x_1} \right)^2 dx_1 + x f_1(\tau) + f_2(\tau). \quad (18)$$

The integration constants $f_1(\tau)$ and $f_2(\tau)$ are obtained, by using boundary conditions (14) and (15) in Equation (18), as

$$f_2(\tau) = 0, \quad (19)$$

and

$$f_1(\tau) = \left(\frac{k_p}{1 + k_p} \right) \frac{\gamma^4}{2} \int_0^1 \left(\frac{\partial w}{\partial x} \right)^2 dx + \frac{\gamma^4}{(1 + k_p)} e_0 \cos 2\Omega \tau, \quad (20)$$

where $e_0 = m\Omega^2 e_1$.

Combining Equations (11), (16), (18–20) and neglecting terms $o(\gamma^4)$, we get

$$\begin{aligned} \frac{\partial^2 w}{\partial \tau^2} + 2c \frac{\partial^2 w}{\partial x \partial \tau} + (kc^2 - T_0 - 2\epsilon e_0(1-k) \cos 2\Omega\tau) \frac{\partial^2 w}{\partial x^2} + \frac{\partial^4 w}{\partial x^4} \\ = k\epsilon \left[\int_0^1 \left(\frac{\partial w}{\partial x} \right)^2 dx \right] \frac{\partial^2 w}{\partial x^2}, \end{aligned} \quad (21)$$

where $\epsilon (= \gamma^2/2)$ will be treated as the small parameter, since $\epsilon \ll 1$.

The following points are at once observed from Equation (21):

- (a) As expected, the spring flexibility makes the system softer.
- (b) For a rigidly mounted pulley (i.e., $k = 1$), the unbalance has no effect. This is because the unbalance force gets balanced by the reactive force at the pulley-support.

A small viscous damping force $\epsilon\mu(\partial w/\partial \tau)$ can then be introduced into Equation (21) which can be recast in the standard state-space form as [18]

$$\mathbf{A} \frac{\partial \mathbf{W}}{\partial \tau} + \mathbf{B} \mathbf{W} = \epsilon \mathbf{N}_1 + \epsilon \mathbf{N}_2, \quad (22)$$

where

$$\begin{aligned} \mathbf{A} = \begin{bmatrix} I & 0 \\ 0 & K \end{bmatrix}, \quad \mathbf{B} = \begin{bmatrix} G & K \\ -K & 0 \end{bmatrix}, \quad \mathbf{W} = \begin{Bmatrix} \frac{\partial w}{\partial \tau} \\ w \end{Bmatrix}, \\ \mathbf{N}_1 = \left\{ 2e_0(1-k) \cos 2\Omega\tau \frac{\partial^2 w}{\partial x^2} - \mu \frac{\partial w}{\partial \tau}, 0 \right\}^T, \end{aligned} \quad (23)$$

and

$$\mathbf{N}_2 = \left\{ k \left(\int_0^1 \left(\frac{\partial w}{\partial x} \right)^2 dx \right) \frac{\partial^2 w}{\partial x^2}, 0 \right\}^T \quad (24)$$

with I as the identity operator, $K \equiv (kc^2 - T_0)(\partial^2/\partial x^2) + (\partial^4/\partial x^4)$, $G \equiv 2c(\partial/\partial x)$.

In the presence of a harmonic excitation, expressed in the non-dimensional form as $f(x) \cos(\Omega_f \tau + \theta_f)$, the equation of motion (22) becomes

$$\mathbf{A} \frac{\partial \mathbf{W}}{\partial \tau} + \mathbf{B} \mathbf{W} = \epsilon \mathbf{N}_1 + \epsilon \mathbf{N}_2 + \mathbf{f}, \quad (25)$$

where

$$\mathbf{f} = \{f(x) \cos(\Omega_f \tau + \theta_f), 0\}^T. \quad (26)$$

3. Brief Review of Non-Linear Complex Normal Modes

In this section, a brief review of the non-linear, complex normal modes for a traveling beam is given [10]. The non-linear complex modes are the free vibration response at a single frequency, including the non-linear effects. For a traveling beam, vibrating in the n th mode, the response is assumed as

$$W(x, \tau) = \frac{a}{2} \Psi_n(x) e^{i\omega_n \tau} + \frac{\bar{a}}{2} \bar{\Psi}_n(x) e^{-i\omega_n \tau},$$

where $\Psi_n = \begin{Bmatrix} i\omega_n \psi_n \\ \psi_n \end{Bmatrix}$ with ψ_n and ω_n as the n th non-linear mode shape and the corresponding frequency, respectively. Both these quantities, however, are amplitude dependent. Here and in the following, a bar above an expression denotes the complex conjugate of the term. Assuming the non-linearity to be small, ω_n and ψ_n are expanded, respectively, as

$$\omega_n = \omega_n^l + \varepsilon \beta_1^{(n)} + \dots, \quad (27)$$

$$\Psi_n = \Phi_n + \varepsilon \Delta_1 + \dots. \quad (28)$$

In Equation (28), $\Phi_n = \begin{Bmatrix} i\omega_n^l \phi_n \\ \phi_n \end{Bmatrix}$, with ϕ_n as the n th linear, complex normal mode of frequency ω_n^l , which are obtained by solving the equation

$$-\omega^2 \phi - 2c\omega \frac{d\phi}{dx} + (kc^2 - T_0) \frac{d^2\phi}{dx^2} + \frac{d^4\phi}{dx^4} = 0, \quad (29)$$

with the boundary conditions

$$\phi(0) = \phi(1) = 0$$

and

$$\frac{d^2\phi(0)}{dx^2} = \frac{d^2\phi(1)}{dx^2} = 0.$$

Furthermore, the vector Φ_n satisfies the following equation:

$$i\omega_n^l \mathbf{A} \Phi_n + \mathbf{B} \Phi_n = \mathbf{0} \quad (30)$$

and the bi-orthogonality relations:

$$\int_0^1 \Phi_m^T \mathbf{A} \Phi_n dx = 0, \quad \text{for all } m \text{ and } n, \quad (31)$$

and

$$\int_0^1 \bar{\Phi}_m^T \mathbf{A} \Phi_n dx = 0, \quad \text{for all } m \neq n. \quad (32)$$

We now use the temporal harmonic balance method after putting $\mathbf{N}_1 = \mathbf{0}$ to get the following equation and its complex conjugate:

$$i\omega_n \frac{a}{2} \mathbf{A} \Psi_n + \frac{a}{2} \mathbf{B} \Psi_n = \varepsilon \mathbf{N}_{2\psi}, \quad (33)$$

where

$$\mathbf{N}_{2\psi} = \left\{ \frac{ka^2\bar{a}}{8} \left[\left(\int_0^1 \left(\frac{d\psi_n}{dx} \right)^2 dx \right) \frac{d^2\bar{\psi}_n}{dx^2} + 2 \left(\int_0^1 \frac{d\psi_n}{dx} \frac{d\bar{\psi}_n}{dx} dx \right) \frac{d^2\psi_n}{dx^2} \right], 0 \right\}^T. \quad (34)$$

A perturbation technique can be applied subsequently, using expansions (27) and (28) together with relations (30–32) to obtain

$$\beta_1^{(n)} = -\frac{\omega_n^l}{4} a\bar{a} \frac{\lambda(\bar{\phi}_n, \phi_n)}{t_n}, \quad (35)$$

$$\Delta_1 = a\bar{a} \left[\sum_{m \neq n} g_m \Phi_m + \sum_{m=1}^{\infty} h_m \bar{\Phi}_m \right], \quad (36)$$

where

$$g_m = -\frac{k}{4} \frac{\omega_m^l}{\omega_n^l - \omega_m^l} \frac{\lambda(\bar{\phi}_m, \phi_n)}{t_n}, \quad m \neq n,$$

$$h_m = \frac{k}{4} \frac{\omega_m^l}{\omega_n^l + \omega_m^l} \frac{\lambda(\phi_m, \phi_n)}{t_n}, \quad m = 1, 2, 3, \dots,$$

$$t_n = \int_0^1 \bar{\Phi}_n^T \mathbf{A} \Phi_n dx, \quad n = 1, 2, 3, \dots,$$

and

$$\lambda(\phi_m, \phi_n) = 2 \left(\int_0^1 \phi_m \frac{d^2\phi_n}{dx^2} dx \right) \left(\int_0^1 \frac{d\phi_n}{dx} \frac{d\bar{\phi}_n}{dx} dx \right) + \left(\int_0^1 \phi_m \frac{d^2\bar{\phi}_n}{dx^2} dx \right) \left(\int_0^1 \left(\frac{d\phi_n}{dx} \right)^2 dx \right).$$

As will be explained in the next section, the non-linear complex normal modes can conveniently be used to get the response of the parametrically excited beam (i.e., when $\mathbf{N}_1 \neq \mathbf{0}$ in Equation (22)).

4. Limit Cycle Amplitude without External Forcing

Assuming that the amplitude of the solution to Equation (22) changes slowly with time, one can write the response as

$$W(x, \tau) = \frac{1}{2} \Lambda_p e^{i\Omega\tau} + \text{c.c.}, \tag{37}$$

with $\Lambda_p = \left\{ \begin{matrix} i\Omega\lambda_p \\ \lambda_p \end{matrix} \right\}$ and λ_p as a complex shape function. The abbreviation c.c. denotes the complex conjugate of the preceding term.

Depending upon the relation between Ω and the linear natural frequencies (ω_n^l) of the traveling beam, different kinds of parametric excitation may appear. In what follows, we analyze only the primary excitation.

In order to study the primary resonance, we set

$$\Omega = \omega_n^l + \varepsilon\sigma_n, \tag{38}$$

where σ_n is called the detuning parameter. In such a situation the n th mode is primarily excited and one can write

$$\Lambda_p = a_n(\tau)\Psi_n + \varepsilon \left[\sum_{m \neq n} a_m(\tau)\Psi_m + \sum_{m=1}^{\infty} b_m(\tau)\bar{\Psi}_m \right]. \tag{39}$$

Further, for a slowly varying amplitude, we write

$$\frac{da_j(\tau)}{d\tau} = o(\varepsilon) = \varepsilon\alpha_j \text{ (say), for } j = 1, 2, \dots, \tag{40}$$

and

$$\frac{db_j(\tau)}{d\tau} = o(\varepsilon) = \varepsilon\delta_j \text{ (say), for } j = 1, 2, \dots$$

Now, first we substitute Equations (37), (38), and (40) into Equation (22). Thereafter, equating the coefficients of $e^{i\Omega\tau}$ from both sides and retaining terms up to the order $o(\varepsilon)$, we get

$$\begin{aligned} &\varepsilon \frac{\alpha_n}{2} \mathbf{A}\Phi_n + i \frac{a_n}{2} (\Omega - \omega_n) \mathbf{A}\Phi_n \\ &+ \varepsilon \left[\sum_{m \neq n} \frac{a_m}{2} (i\Omega \mathbf{A}\Phi_m + \mathbf{B}\Phi_m) + \sum_{m=1}^{\infty} \frac{b_m}{2} (i\Omega \mathbf{A}\bar{\Phi}_m + \mathbf{B}\bar{\Phi}_m) \right] = \varepsilon \mathbf{N}'_1, \end{aligned} \tag{41}$$

where

$$\mathbf{N}'_1 = \left\{ e_0(1-k) \frac{d^2 \bar{\phi}_n}{dx^2} \frac{\bar{a}_n}{2} - i\Omega\mu\phi_n \frac{a_n}{2}, 0 \right\}^T.$$

It is to be noted that, while deriving Equation (41), the fact that $(\Omega - \omega_n)$ is $o(\varepsilon)$, as can easily be seen from Equations (39) and (27), has been made use of.

By using Equations (31) and (32) in Equation (41) one gets

$$\varepsilon\alpha_n + ia_n(\Omega - \omega_n) = \frac{2\varepsilon \int_0^1 \bar{\Phi}_n^T \mathbf{N}'_1 dx}{t_n}. \tag{42}$$

For notational simplicity, we shall replace a_n by a , and express the complex amplitude a as

$$a = \tilde{a}e^{i\theta}, \tag{43}$$

with \tilde{a} as real.

Using Equations (27), (35), (38), (40), and (43) in Equation (42) and thereafter separating the real and imaginary parts, we get

$$\frac{d\tilde{a}}{d\tau} = -\varepsilon e'_0 \tilde{a} [G^I \cos 2\theta - G^R \sin 2\theta] - \varepsilon \mu' \tilde{a}, \quad (44)$$

and

$$\tilde{a} \frac{d\theta}{d\tau} = \varepsilon \frac{\tilde{a}^3}{4} \frac{\omega_n^I}{t_n} d_n - \varepsilon \tilde{a} \sigma_n + \varepsilon e'_0 \tilde{a} [G^R \cos 2\theta + G^I \sin 2\theta], \quad (45)$$

where

$$d_n = k \left[\left(\int_0^1 \left(\frac{d\phi_n}{dx} \right)^2 dx \right) \left(\int_0^1 \left(\frac{d\bar{\phi}_n}{dx} \right)^2 dx \right) + 2 \left(\int_0^1 \frac{d\phi_n}{dx} \frac{d\bar{\phi}_n}{dx} dx \right)^2 \right],$$

$$G = G^R + iG^I = \int_0^1 \left(\frac{d\bar{\phi}_n}{dx} \right)^2 dx,$$

$$H = \int_0^1 \phi_n \bar{\phi}_n dx,$$

$$e'_0 = \frac{e_0 \omega_n^I (1-k)}{t_n},$$

and

$$\mu' = \frac{\mu (\omega_n^I)^2 H}{t_n}. \quad (46)$$

The steady-state solutions correspond to the fixed points of Equations (44) and (45) and are obtained by putting

$$\frac{d\tilde{a}}{d\tau} = 0 \quad \text{and} \quad \frac{d\theta}{d\tau} = 0 \quad (\text{if } \tilde{a} \neq 0). \quad (47)$$

A ready inspection reveals that $\tilde{a} = 0$ is a fixed point, which is called the 'trivial limit cycle' in the literature [5]. The amplitude (\tilde{a}) and the phase angle (θ) of non-trivial limit cycle(s) are obtained from Equations (44–47). In this way, we finally obtain

$$\sin(2\theta - \delta) = \frac{\mu'}{e'_0 \sqrt{(G^R)^2 + (G^I)^2}}, \quad (48)$$

$$\cos(2\theta - \delta) = \frac{1}{e'_0 \sqrt{(G^R)^2 + (G^I)^2}} \left[\sigma_n - \frac{\tilde{a}^2}{4} \frac{\omega_n^I}{t_n} d_n \right], \quad (49)$$

with

$$\delta = \arctan \left(\frac{G^I}{G^R} \right).$$

Squaring and adding Equations (48) and (49), one gets

$$(\tilde{a}\sqrt{\varepsilon})^2 = \frac{4t_n}{\omega_n^2 d_n} \left[\varepsilon\sigma_n \pm \sqrt{(\varepsilon e'_0)^2 [(G^R)^2 + (G^I)^2] - (\varepsilon\mu')^2} \right]. \quad (50)$$

Remembering that \tilde{a}^2 should be positive, it is easy to note the following three possibilities from Equation (50):

(a) No non-trivial limit cycle exists:

(i) if

$$e'_0 < \frac{\mu'}{\sqrt{(G^R)^2 + (G^I)^2}}, \quad (51)$$

(ii) even if condition (51) is violated but $\sigma_n < 0$ and

$$|\sigma_n| > \sqrt{e_0'^2 (G^R)^2 + (G^I)^2 - \mu'^2}. \quad (52)$$

(b) Only one limit cycle exists, if condition (51) is violated and

$$|\sigma_n| < \sqrt{e_0'^2 (G^R)^2 + (G^I)^2 - \mu'^2}. \quad (53)$$

(c) Two limit cycles exist, if both conditions (51) and (53) are violated for $\sigma_n > 0$.

It must be emphasized that even if a non-trivial limit cycle exists, it may not be stable. The analysis detailed below is then required to confirm the stability of the limit cycle.

4.1. STABILITY ANALYSIS OF LIMIT CYCLES

The stability of the limit cycle(s), obtained in Section 4, is determined by linearizing Equation (42) about the fixed points of \tilde{a} and θ . Since for the trivial limit cycle ($\tilde{a} = 0$) no unique phase angle (θ) exists, the linear part of Equation (42) is analyzed rather than using Equations (44) and (45). However, for non-trivial limit cycles, linearization of Equations (44) and (45) are carried out around \tilde{a} and θ , given by Equations (48) and (49). In what follows, first we discuss the stability of the trivial limit cycle and then that of the non-trivial one.

4.1.1. Trivial Limit Cycle

We expand a as

$$a = a_x + ia_y. \quad (54)$$

Putting Equations (28) and (54) in Equation (42), we get by neglecting the non-linear terms and equating the real and imaginary parts separately from both sides

$$\frac{d}{d\tau} \begin{Bmatrix} a_x \\ a_y \end{Bmatrix} = \varepsilon \begin{bmatrix} (C - D) & (E - F) \\ -(E + F) & -(C + D) \end{bmatrix} \begin{Bmatrix} a_x \\ a_y \end{Bmatrix}, \quad (55)$$

where $C = e'_0 G^I$, $D = \mu'$, $E = \sigma_n$, $F = e'_0 G^R$.

The eigenvalues of the coefficient matrix are then given by

$$s_{1,2} = -D \pm \sqrt{D^2 + [(C^2 - D^2) - (E^2 - F^2)]},$$

which implies that the trivial limit cycle is unstable if

$$\sigma_n^2 < [e_0'^2 ((G^I)^2 + (G^R)^2) - \mu'^2]. \quad (56)$$

Comparing condition (56) with conditions (51–53), it is inferred that the trivial limit cycle is stable, if this is the only limit cycle or if two more non-trivial limit cycles exist. However, the trivial limit cycle is unstable, if there exists only one more non-trivial limit cycle.

4.1.2. Non-Trivial Limit Cycle

To ascertain the stability of the non-trivial limit cycles, one perturbs the amplitude (\tilde{a}) and phase (θ) in Equations (44) and (45) in the form

$$\tilde{a}_p = \tilde{a} + \eta_p \quad (57)$$

and

$$\theta_p = \theta + \zeta_p. \quad (58)$$

Substituting Equations (57) and (58) into Equations (44) and (45) and using Equations (48–50), we obtain the following (after linearization):

$$\frac{d}{d\tau} \begin{Bmatrix} \eta_p \\ \zeta_p \end{Bmatrix} = \varepsilon \begin{bmatrix} 0 & 2e'_0 \tilde{a} \sqrt{(G^R)^2 + (G^I)^2} \cos(2\theta - \delta) \\ \frac{1}{2} \frac{\omega_n^l d_n}{t_n} \tilde{a} & -2\mu' \end{bmatrix} \begin{Bmatrix} \eta_p \\ \zeta_p \end{Bmatrix}. \quad (59)$$

The eigenvalues of the coefficient matrix of Equation (59) are

$$s_{1,2} = -\mu' \pm \sqrt{\mu'^2 + e'_0 \frac{\omega_n^l d_n}{t_n} \tilde{a}^2 [(G^R)^2 + (G^I)^2]^{1/2} \cos(2\theta - \delta)}. \quad (60)$$

From Equation (60) one can show that the limit cycle is stable if $\cos(2\theta - \delta) < 0$. From Equations (48) and (49) and conditions (51–53) one can conclude:

- (i) When two non-trivial limit cycles exist, the value of $\cos(2\theta - \delta)$ is negative for the limit cycle with the larger amplitude and positive for the one with the smaller amplitude. Hence the limit cycle with the larger amplitude is stable and the other one unstable.
- (ii) When a single non-trivial limit cycle exists, it is always stable because the value of $\cos(2\theta - \delta)$ associated with it is negative.

4.2. NUMERICAL RESULTS AND DISCUSSIONS

Numerical results are presented to show the effects of various system parameters on the steady-state solution, i.e., the amplitude of the limit cycle. All the results have been obtained with $T_0 = 1$. We shall concentrate on the effects of only those parameters which can be independently controlled. These parameters are defined below:

- (i) The axial speed of the beam, expressed as a speed parameter $c' = c/c_{cr}$ where $c_{cr} = \sqrt{T_0 + \pi^2}$. It may be noted that c' varies linearly with both Ω and R , as $c' = 2\Omega R / \sqrt{T_0 + \pi^2}$.
- (ii) The stiffness of the flexible pulley-support designated by the non-dimensional parameter k .
- (iii) The amount of unbalance me_1 , generating the parametric excitation, expressed by the non-dimensional parameter εe_0 .
- (iv) The external damping parameter $\varepsilon\mu$.

For the primary parametric excitation, Ω should be in the neighbourhood of ω_n^l , which in turn depends on various system parameters, like c' and k . The results are, therefore, obtained for

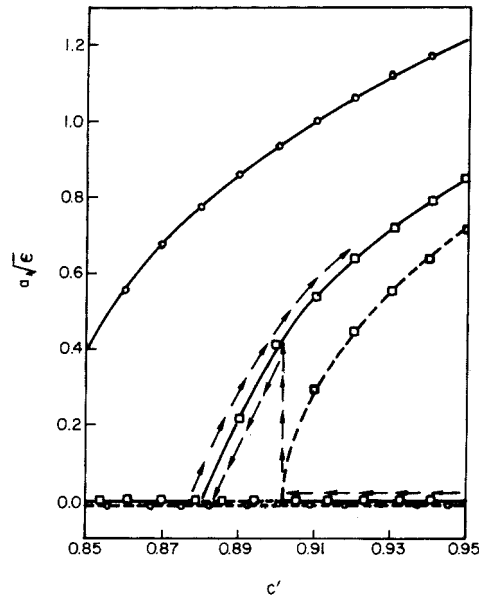


Figure 2. Variation of the limit-cycle amplitudes with c' . $R = 0.2$, $k = 0.5$, $\varepsilon\mu = 0.05$; \circ : $\varepsilon e_0 = 0.8$, \square : $\varepsilon e_0 = 0.1$; — stable, - - - unstable.

the ranges of values of c' and k , that yield $\omega_n^l \simeq \Omega$. Further, results are presented for $n = 1$, i.e., when the first mode is primarily excited through the parametric excitation.

Figure 2 shows the variation of the limit cycle amplitudes with the axial speed for two different values of εe_0 . It is indicated, as discussed earlier in Section 4.1, that when two limit cycles exist, the trivial one is unstable. On the other hand, when three limit cycles exist, the trivial one and the one with the highest amplitude are stable. The amplitudes of the non-trivial and stable limit cycles are seen to increase with increasing axial speed. Moreover, if three limit cycles exist, then a jump phenomenon with decreasing axial speed occurs, as exhibited in Figure 2. This feature has also been exhibited by a parametrically excited Duffing oscillator, as reported in [5]. Similar observations were also made by varying the stiffness parameter k .

Figure 3 shows the effect of variation of the unbalance parameter εe_0 for two different axial speeds. At the lower speed, for which σ_n is negative, only the trivial limit cycle exists for low values of εe_0 . With increasing εe_0 , beyond a critical value, two limit cycles appear. When the axial speed is increased beyond a critical value, σ_n becomes positive. In such a situation, one, two or three limit cycles may exist depending on the value of εe_0 . At such high speeds, the possibility of a two-way jump phenomenon, as εe_0 changes, is clearly indicated in Figure 3.

Figure 4 shows the effect of the external damping parameter at three different axial speeds. It may be noted, that with increasing damping, the non-trivial limit cycle vanishes at all speeds. The jump phenomenon is also exhibited as the damping parameter changes. Both one-way and two-way jumps are possible depending on the axial speed.

Let us now summarize the effects of the non-linearity on the stability of an axially moving beam which is parametrically excited. To this end we draw Figure 5, spanning a region in the parameter space, where the parameters used are defined in Sections 4 and 4.1. Using Equation (56) one can draw the curve AB delineating the stable and unstable zones as predicted by the linear analysis, where the zone marked II refers to the unstable zone. When the non-linearities are included, in the zone marked I, the equilibrium position turns out to be stable,

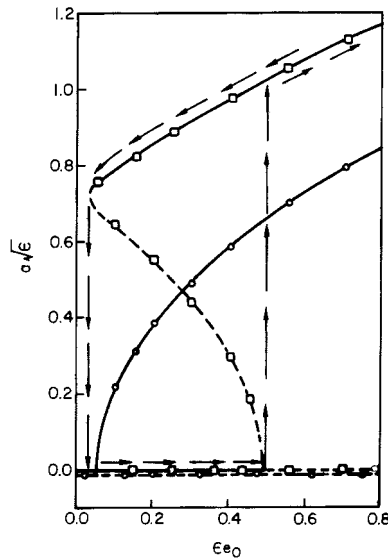


Figure 3. Variation of the limit-cycle amplitudes with $\epsilon\epsilon_0$. $R = 0.2$, $k = 0.5$, $\epsilon\mu = 0.05$; \circ : $c' = 0.89$, \square : $c' = 0.94$; — stable, - - - unstable.

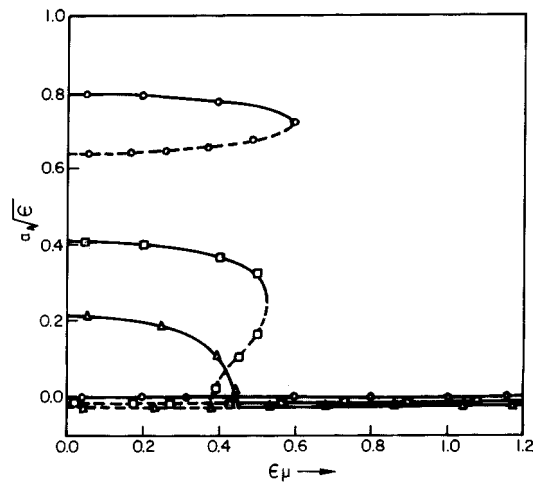


Figure 4. Variation of the limit-cycle amplitudes with $\epsilon\mu$. $R = 0.2$, $k = 0.5$, $\epsilon\epsilon_0 = 0.1$; \circ : $c' = 0.94$, \square : $c' = 0.90$, \triangle : $c' = 0.89$; — stable, - - - unstable.

whereas in zone II the equilibrium position becomes unstable and a stable limit cycle (with finite amplitude) is approached. However, in the zone marked III, the system approaches either the equilibrium position or a stable limit cycle depending on the initial disturbance.

5. Near-Resonance Response with Simultaneous Parametric and Harmonic Excitations

In this section, the response $w(x, \tau)$ is obtained when an external harmonic force is present over and above the parametric excitation. Because of the presence of both the excitations, the response usually turns out to be aperiodic. It is to be noted that different combinations of frequencies of parametric and harmonic excitations are possible. These, in turn, may give

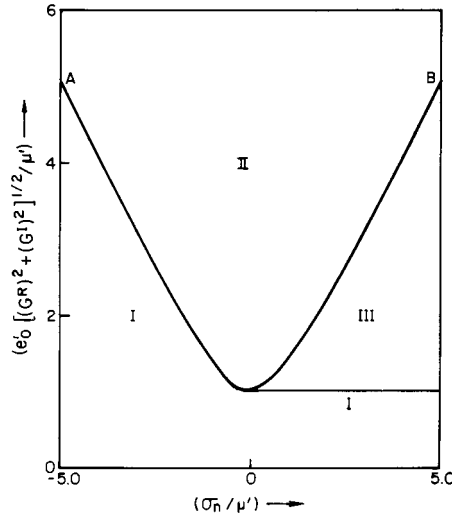


Figure 5. Stability boundaries of the parametrically excited system as predicted by the linear analysis.

rise to various complex patterns of the response. In what follows we shall consider a special case, where the exciting frequency is close to the natural frequency associated with the mode excited by the parametric excitation. Hence, along with Equation (39) we also assume that the forcing frequency Ω_f is given by

$$\Omega_f = \omega_n^l + \varepsilon\sigma. \quad (61)$$

When $\sigma_n \neq \sigma$, the response is almost periodic. In the absence of any parametric excitation, the steady-state response is also harmonic having the same frequency as that of the excitation. But in the presence of a small parametric excitation, the response can be assumed as

$$W(x, \tau) = \sum_{n=1}^{\infty} \frac{a_n(\tau)}{2} \Psi_n e^{i\Omega_f \tau} + \text{c.c.} \quad (62)$$

In view of Equations (37) and (61), the following assumptions are justified:

$$a_m = \varepsilon a'_m \quad \text{for } m \neq n, \quad (63)$$

and

$$\bar{a}_m = \varepsilon \bar{a}'_m \quad \text{for } m = 1, 2, 3, \dots, \quad (64)$$

with

$$\frac{d}{d\tau} a_n(\tau) = o(\varepsilon). \quad (65)$$

We now substitute Equations (62–65) into Equation (25) and balance the harmonics (i.e., equate the coefficients of $e^{i\Omega_f \tau}$ and $e^{-i\Omega_f \tau}$ separately, from both sides of the equation). Then using Equations (33) and (34) and retaining terms up to $o(\varepsilon)$, we get

$$\begin{aligned} & \frac{1}{2} \frac{da_n}{d\tau} \mathbf{A}\Psi_n + i(\Omega_f - \omega_n) \frac{a_n}{2} \mathbf{A}\Psi_n \\ & + \varepsilon \left[\sum_{m \neq n} i \frac{a'_m}{2} (\Omega_f - \omega_m^l) \mathbf{A}\Phi_m + \sum_{m=1}^{\infty} i \frac{\bar{a}'_m}{2} (\Omega_f + \omega_m^l) \mathbf{A}\bar{\Phi}_m \right] = \varepsilon \mathbf{N}_f + \mathbf{f}_1, \quad (66) \end{aligned}$$

where

$$\mathbf{N}_f = \left\{ e_0(1-k) \frac{d^2 \bar{\phi}_n}{dx^2} e^{2i\varepsilon(\sigma_n - \sigma)\tau} \frac{\bar{a}_n}{2} - i\omega_n^l \mu \phi_n \frac{a_n}{2}, 0 \right\}^T, \quad (67)$$

and

$$\mathbf{f}_1 = \left\{ \frac{f(x)}{2} e^{i\theta_f}, 0 \right\}^T. \quad (68)$$

Using Equation (65) and bi-orthogonality relations (31) and (32) in Equation (66), and by retaining terms up to $o(\varepsilon)$, we get

$$\frac{da_n}{d\tau} + ia_n(\Omega_f - \omega_n) = \frac{2\varepsilon}{t_n} \int_0^1 \bar{\Phi}_n^T \mathbf{N}_f dx + \frac{2}{t_n} \int_0^1 \bar{\Psi}_n^T \mathbf{f}_1 dx. \quad (69)$$

Further, the coefficients a'_m and \bar{a}'_m 's can be obtained as

$$\varepsilon a'_m = a_m = \frac{2 \int_0^1 \bar{\Phi}_m^T (\mathbf{f}_1 + \varepsilon \mathbf{N}_f) dx}{i(\Omega_f - \omega_m^l) t_m} \quad \text{if } m \neq n, \quad (70)$$

and

$$\varepsilon \bar{a}'_m = \bar{a}_m = \frac{2 \int_0^1 \Phi_m^T (\mathbf{f}_1 + \varepsilon \mathbf{N}_f) dx}{i(\Omega_f + \omega_m^l) t_m} \quad \text{for } m = 1, 2, \dots \quad (71)$$

Since \mathbf{N}_f contains a term having explicit time dependence, Equation (69) does not exhibit any periodic solution unless $\sigma_n = \sigma$. Let us consider the special case when $\sigma_n = \sigma$, i.e., the frequencies of the parametric and external excitations are the same. In this case, a steady-state solution to Equation (69) exists. This solution can be obtained as explained below.

Substitution of $(da_n)/(d\tau) = 0$ in Equation (69) yields the complex algebraic equation

$$ia_n(\Omega_f - \omega_n) = \frac{2\varepsilon}{t_n} \int_0^1 \bar{\Phi}_n^T \mathbf{N}_f dx + \frac{2}{t_n} \int_0^1 \bar{\Psi}_n^T \mathbf{f}_1 dx. \quad (72)$$

For solving Equation (72) to determine a_n , we substitute $a_n = \tilde{a}_n e^{i\theta_n}$ in the above equation and equate the real and imaginary parts from both sides to obtain

$$\begin{aligned} \tilde{a}_n(\Omega_f - \omega_n^l - \varepsilon \tilde{a}_n^2 \beta_1^{(n)}) \cos \theta_n &= \varepsilon e'_0 \tilde{a}_n [G^R \cos \theta_n + G^I \sin \theta_n] \\ &\quad - \varepsilon \mu' \tilde{a}_n \sin \theta_n + \frac{1}{t_n} [Q^R + \varepsilon \tilde{a}_n^2 M^R], \end{aligned} \quad (73)$$

and

$$\begin{aligned} \tilde{a}_n(\Omega_f - \omega_n^l - \varepsilon \tilde{a}_n^2 \beta_1^{(n)}) \sin \theta_n &= \varepsilon e'_0 \tilde{a}_n [G^I \cos \theta_n - G^R \sin \theta_n] \\ &\quad + \varepsilon \mu' \tilde{a}_n \cos \theta_n + \frac{1}{t_n} [Q^I + \varepsilon \tilde{a}_n^2 M^I], \end{aligned} \quad (74)$$

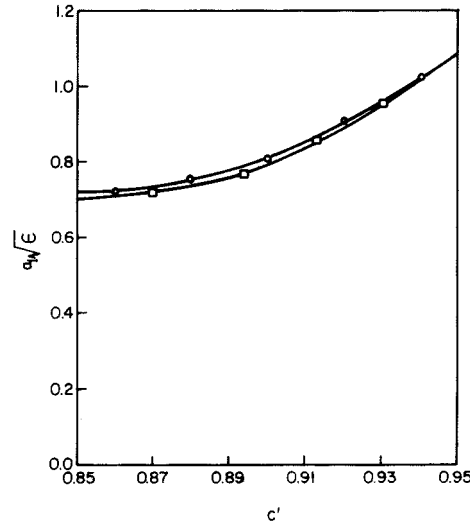


Figure 6a. Variation of the roots of Equations (73) and (74) with c' . $R = 0.2$, $k = 0.5$, $\theta_f = 0.0$, $\epsilon\mu = 0.05$, $F_0\sqrt{\epsilon} = 10.0$; \circ : $\epsilon\epsilon_0 = 0.8$, \square : $\epsilon\epsilon_0 = 0.1$.

where

$$Q = Q^R + iQ^I = -\omega_n^l \int_0^1 \bar{\phi}_n f e^{i\theta_f} dx$$

and

$$M = M^R + iM^I = \left\{ -\sum_{m \neq n} \bar{g}_m \omega_m^l \int_0^1 \bar{\phi}_m f e^{i\theta_f} dx \right\} + \left\{ \sum_{m=1}^{\infty} \bar{h}_m \omega_m^l \int_0^1 \phi_m f e^{i\theta_f} dx \right\}.$$

Now eliminating θ_n from Equations (73) and (74) one gets, after some algebraic manipulations, a quintic polynomial in \tilde{a}_n^2 . This polynomial for a concentrated external force (at $x = x_0$), i.e., when $f(x)$ in Equation (26) is written as $F_0\delta(x - x_0)$, is given in Appendix II. For this particular loading, numerical results reveal one, three or five (positive) values of \tilde{a}_n^2 . However, a subsequent stability analysis only can confirm whether the values so obtained are physically realizable (i.e., stable) or not.

The stability analysis can be carried out by using the method outlined in Section 4.1. However, an alternative procedure, considering an arbitrary perturbation to the solution, which gives rise to Mathieu type equation, has been carried out. The details of the stability analysis considering only the primary instability are outlined in Appendix III. This method can also be extended to capture the higher order instabilities as well.

5.1. NUMERICAL RESULTS AND DISCUSSIONS

In this section, numerical results are presented to study the effects of several parameters on the steady-state response. All the results are obtained for $T_0 = 1$, $x_0 = 1/3$ and $\Omega_f \simeq \Omega \simeq \omega_1^l$.

At this stage it should be noted from Equations (62–64) that the steady-state response of the beam is obtained (up to $o(1)$) as

$$w(x, \tau) = \tilde{a}_1 \phi_1(x) \cos(\Omega_f \tau + \theta_1 + \rho_1),$$

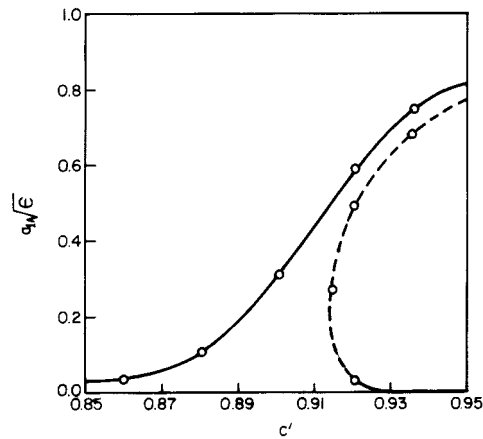


Figure 6b. Variation of the roots of Equations (73) and (74) with c' . $R = 0.2$, $k = 0.5$, $\theta_f = 0.0$, $\varepsilon\mu = 0.05$, $F_0\sqrt{\varepsilon} = 0.1$; \circ : $\varepsilon e_0 = 0.1$; — stable, - - - unstable.

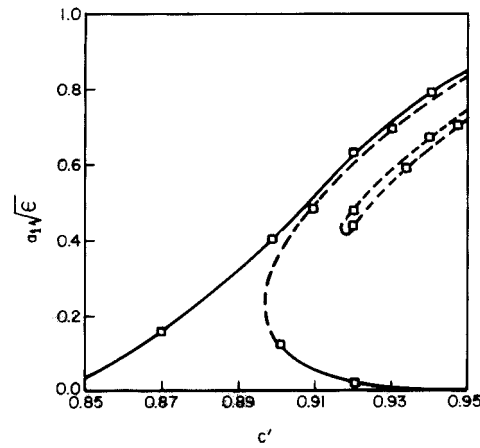


Figure 6c. Variation of the roots of Equations (73) and (74) with c' . $R = 0.2$, $k = 0.5$, $\theta_f = 0.0$, $\varepsilon\mu = 0.05$, $F_0\sqrt{\varepsilon} = 0.1$; \square : $\varepsilon e_0 = 0.8$; — stable, - - - unstable.

where $\tan \rho_1 = -\phi_1^I/\phi_1^R$, $\phi_1 = \sqrt{(\phi_1^R)^2 + (\phi_1^I)^2}$. The values of \tilde{a}_1 and θ_1 are now obtained by solving Equations (73) and (74). Subsequently, we study how the different parameters affect the value of \tilde{a}_1 .

Figures 6a–6c show the response variable \tilde{a}_1 with increasing speed for two different sets of values of F_0 and εe_0 . It is seen from Figure 6a that if the external forcing predominates, then only one stable response is resulted. The value of \tilde{a}_1 , while remaining insensitive to the amount of unbalance, increases with increasing speed. On the other hand, if the parametric excitation predominates, then depending on the value of εe_0 and c' , one or three unstable roots for \tilde{a}_1 may be obtained (Figures 6b and 6c). However, the common jump phenomenon, observed in a harmonically forced Duffing oscillator, is not altered. Figure 7 clearly indicates that, if a flexible pulley-support is used, then the steady-state response can be controlled by adjusting the phase difference (between the external and parametric excitations) θ_f .

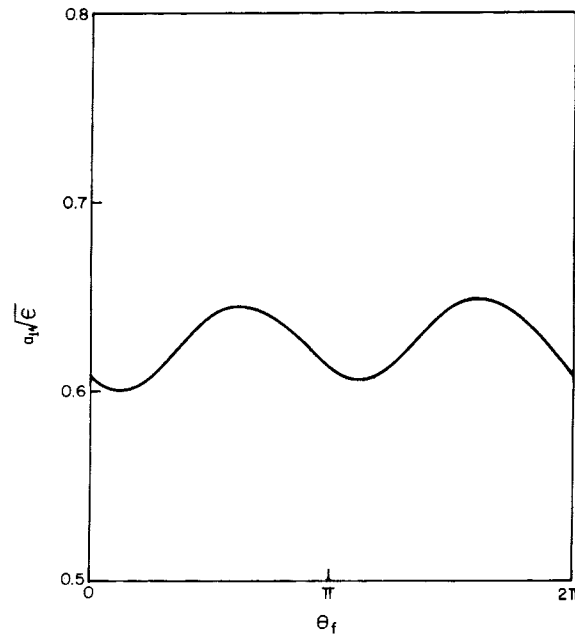


Figure 7. Variation of the roots of Equations (73) and (74) with phase difference (θ_f). $R = 0.2$, $k = 0.5$, $c' = 0.85$, $\varepsilon\mu = 0.05$, $F_0\sqrt{\varepsilon} = 10.0$, $\varepsilon e_0 = 0.8$; — stable, - - - unstable.

6. Conclusions

In the present work, non-linear, complex, normal modes have been used to study the response of a parametrically excited traveling beam both without and with an external harmonic forcing. The primary parametric resonance, in the absence of external forcing, has been analyzed. The effects of the non-linearity are clearly brought out. The limit cycles which appear only after including the non-linearity have been investigated. It has been shown that the amplitudes of limit cycles exhibit both 'one-way' and 'two-way' jump phenomena which are very similar to those observed in a parametrically excited Duffing oscillator.

For a parametrically excited traveling beam with an external harmonic excitation, the effects of various system parameters depend on the relative strengths of the two forms of excitation. Moreover, a particular phase difference between the two excitations results in the minimum value of the steady-state response.

Appendix I: List of Symbols

w^*	= transverse displacement of the beam
u^*	= longitudinal displacement of the beam
c^*	= uniform axial speed
T_0^*	= initial tension in the beam
k_p^*	= spring stiffness of the pulley
m^*	= eccentric unbalanced mass
e_1^*	= eccentricity of the unbalanced mass
$2\Omega^*$	= rotational speed of the pulley
R^*	= pulley radius

ρ	= density of the beam material
E	= Young's modulus of the beam material
A	= area of cross-section of the beam
l	= length of the beam
I_z	= second moment of area of cross section about the neutral axis
r	= radius of gyration of the beam cross-section = $\sqrt{I_z/A}$
γ	= slenderness ratio, $r/l \ll 1$
ε	= $\gamma^2/2$
ξ	= longitudinal distance of a point on the beam from the left support
t	= time
x	= non-dimensional distance
τ	= non-dimensional time
w	= non-dimensional transverse displacement
u	= non-dimensional longitudinal displacement
c	= non-dimensional axial speed
c'	= $c/\sqrt{T_0 + \pi^2}$
T_0	= non-dimensional tension
k_p	= non-dimensional pulley-support stiffness
k	= $k_p/(1 + k_p)$ ($0 \leq k \leq 1$)
m	= non-dimensional pulley unbalance
e_1	= non-dimensional eccentricity
R	= non-dimensional pulley radius
2Ω	= non-dimensional pulley rotational speed
f	= non-dimensional transverse force per unit length
Ω_f	= non-dimensional frequency of excitation
θ_f	= phase difference between two forms of excitation
ϕ_n	= n th linear non-stationary complex normal mode = $\phi_n^R + i\phi_n^I$
i	= $\sqrt{-1}$
ω_n^I	= linear natural frequency of the n th linear mode
ψ_n	= the n th non-linear complex normal mode = $\psi_n^R + i\psi_n^I$
ω_n	= frequency corresponding to the n th non-linear normal mode
ϕ_n^*	= $\sqrt{(\phi_n^R)^2 + (\phi_n^I)^2}$
a_n	= participation of the n th non-linear normal mode = $\tilde{a}_n e^{i\theta_n}$ with \tilde{a}_n as real

Appendix II: Algebraic Equation for Obtaining the Near-Resonance Response

The final algebraic equation, after eliminating θ_n from Equations (74) and (76) for $f(x) = F_0\delta(x - x_0)$, is obtained as

$$\begin{aligned}
 A^5 + A^4 \left[-\frac{4(\Omega_f - \omega_n^I)}{\beta_1^{(n)}} - \nu \{ (M_1^R)^2 + (M_1^I)^2 \} \right] + A^3 \left[\frac{4(\Omega_f - \omega_n^I)^2}{(\beta_1^{(n)})^2} \right. \\
 \left. + \frac{2l_1}{(\beta_1^{(n)})^2} - 2\nu(Q_1^R M_1^R + Q_1^I M_1^I) + \frac{2\nu}{\beta_1^{(n)}} \{ (M_1^R)^2 l_2 + (M_1^I)^2 l_3 \} \right]
 \end{aligned}$$

$$\begin{aligned}
 & + 2\nu \frac{M_1^R M_1^I}{\beta_1^{(n)}} (l_5 - l_4) \Big] + A^2 \left[-\frac{4(\Omega_f - \omega_n^l)l_1}{(\beta_1^{(n)})^3} - \nu \{ (Q_1^R)^2 + (Q_1^I)^2 \} \right. \\
 & - \frac{\nu}{(\beta_1^{(n)})^2} \{ l_2^2 (M_1^R)^2 + l_3^2 (M_1^I)^2 + l_4^2 (M_1^I)^2 + l_5^2 (M_1^R)^2 \} \\
 & + \frac{4\nu}{\beta_1^{(n)}} (l_2 Q_1^R M_1^R + l_3 Q_1^I M_1^I) + \frac{2\nu}{(\beta_1^{(n)})^2} M_1^R M_1^I (l_4 l_2 - l_5 l_3) \\
 & + \frac{2\nu}{\beta_1^{(n)}} (l_5 - l_4) (M_1^R Q_1^I + Q_1^R M_1^I) \Big] + A \left[\frac{l_1^2}{(\beta_1^{(n)})^4} + \frac{2\nu}{\beta_1^{(n)}} \{ l_2 (Q_1^R)^2 + l_3 (Q_1^I)^2 \} \right. \\
 & - \frac{2\nu}{(\beta_1^{(n)})^2} Q_1^R M_1^R (l_2^2 + l_5^2) - \frac{2\nu}{(\beta_1^{(n)})^2} Q_1^I M_1^I (l_4^2 + l_3^2) \\
 & + \left. \frac{2\nu}{\beta_1^{(n)}} Q_1^I Q_1^R (l_5 - l_4) + \frac{2\nu}{(\beta_1^{(n)})^2} (Q_1^I M_1^R + Q_1^R M_1^I) (l_2 l_4 - l_5 l_3) \right] \\
 & + \left[-\frac{\nu}{(\beta_1^{(n)})^2} \{ (Q_1^R)^2 (l_2^2 + l_5^2) + (Q_1^I)^2 (l_4^2 + l_3^2) - 2Q_1^R Q_1^I (l_2 l_4 - l_3 l_5) \} \right] = 0, \quad (75)
 \end{aligned}$$

where

$$\begin{aligned}
 M_1 &= M/F_0, \quad Q_1 = Q/F_0, \quad A = \varepsilon \tilde{a}_n^2, \\
 l_1 &= (\Omega_f - \omega_n^l)^2 - \varepsilon^2 e_0^2 [(G^R)^2 + (G^I)^2] + \varepsilon^2 \mu'^2, \\
 l_2 &= (\Omega_f - \omega_n^l) + \varepsilon e_0' G^R, \quad l_3 = (\Omega_f - \omega_n^l) - \varepsilon e_0' G^R, \\
 l_4 &= \varepsilon \mu' - \varepsilon e_0' G^I, \quad l_5 = \varepsilon \mu' + \varepsilon e_0' G^I, \quad \nu = \left(\frac{F_0}{t_n \beta_1^{(n)}} \right)^2 \varepsilon.
 \end{aligned}$$

Appendix III: Stability Analysis of the Steady-State Solution

The stability of the steady-state solution, given by Equation (69), is studied by perturbing it in the form

$$w_p(x, \tau) = w(x, \tau) + w_\delta(x, \tau). \quad (76)$$

Putting Equation (76) into Equation (25) and neglecting terms of order higher than $o(\varepsilon)$, we get

$$\mathbf{A} \frac{\partial W_\delta}{\partial \tau} + \mathbf{B} W_\delta = \varepsilon \mathbf{N}_{1\delta} + \varepsilon \mathbf{N}_{2\delta}, \quad (77)$$

where

$$W_\delta = \left\{ \begin{array}{c} \frac{\partial w_\delta}{\partial \tau} \\ w_\delta \end{array} \right\},$$

$$\mathbf{N}_{1\delta} = \left\{ 2e_0(1-k) \cos 2\Omega\tau \frac{\partial^2 w_\delta}{\partial x^2} - \mu \frac{\partial w_\delta}{\partial \tau}, 0 \right\}^T \quad (78)$$

and

$$\mathbf{N}_{2\delta} = \left\{ k \left[\left(\int_0^1 \left(\frac{\partial w}{\partial x} \right)^2 dx \right) \frac{\partial^2 w_\delta}{\partial x^2} + 2 \left(\int_0^1 \frac{\partial w}{\partial x} \frac{\partial w_\delta}{\partial x} dx \right) \frac{\partial^2 w}{\partial x^2} \right], 0 \right\}^T. \quad (79)$$

To analyze the stability of a_n , when $\Omega_f = \omega_n^l + \varepsilon\sigma$, the following perturbation is considered:

$$W_\delta = \Phi_n(x)\xi_n(\tau) + \text{c.c.} \quad (80)$$

Substituting the value of $w(x, \tau)$ from Equations (62–64) one gets

$$\mathbf{A}\Phi_n \frac{d\xi_n}{d\tau} + \mathbf{B}\Phi_n \xi_n + \text{c.c.} = \varepsilon \mathbf{L}_1 + \varepsilon \mathbf{L}_2 + \varepsilon \mathbf{L}_3 \frac{d\xi_n}{d\tau} + \text{c.c.}, \quad (81)$$

where

$$\mathbf{L}_j = \{l_j(x, \tau), 0\}^T, \quad j = 1, 2, 3,$$

with

$$\begin{aligned} l_1(x, \tau) = & \frac{k}{4} \tilde{a}_n^2 \left\{ 3 \left(\int_0^1 \left(\frac{d\phi_n}{dx} \right)^2 dx \right) \frac{d^2 \phi_n}{dx^2} \right\} e^{2i(\Omega\tau + \theta_n)} \\ & + \frac{k}{4} \tilde{a}_n^2 \left\{ \left(\int_0^1 \left(\frac{d\bar{\phi}_n}{dx} \right)^2 dx \right) \frac{d^2 \phi_n}{dx^2} + 2 \left(\int_0^1 \frac{d\bar{\phi}_n}{dx} \frac{d\phi_n}{dx} dx \right) \frac{d^2 \bar{\phi}_n}{dx^2} \right\} e^{-2i(\Omega\tau + \theta_n)} \\ & + \frac{k}{4} \tilde{a}_n^2 \left\{ 2 \left(\int_0^1 \left(\frac{d\phi_n}{dx} \right)^2 dx \right) \frac{d^2 \bar{\phi}_n}{dx^2} + 4 \left(\int_0^1 \frac{d\bar{\phi}_n}{dx} \frac{d\phi_n}{dx} dx \right) \frac{d^2 \phi_n}{dx^2} \right\}, \end{aligned}$$

$$l_2(x, \tau) = 2e_0(1-k) \cos 2\Omega\tau \frac{d^2 \phi_n}{dx^2}$$

and

$$l_3(x, \tau) = -\mu \phi_n.$$

Applying the bi-orthogonality relations (i.e., Equations (30) and (31)) and Equation (29), one finally gets the following equation and its complex conjugate:

$$\begin{aligned} \frac{d\xi_n}{d\tau} - i\omega_n^l \xi_n = & \frac{\varepsilon}{t_n} \left(\int_0^1 \bar{\Phi}_n^T (\mathbf{L}_1 + \mathbf{L}_2) dx \right) \xi_n + \frac{\varepsilon}{t_n} \left(\int_0^1 \bar{\Phi}_n^T \mathbf{L}_3 dx \right) \frac{d\xi_n}{d\tau} \\ & + \frac{\varepsilon}{t_n} \left(\int_0^1 \bar{\Phi}_n^T (\bar{\mathbf{L}}_1 + \bar{\mathbf{L}}_2) dx \right) \bar{\xi}_n + \frac{\varepsilon}{t_n} \left(\int_0^1 \bar{\Phi}_n^T \bar{\mathbf{L}}_3 dx \right) \frac{d\bar{\xi}_n}{d\tau}. \end{aligned} \quad (82)$$

Assuming that $\tau' = \Omega_f \tau + \theta_n$ and $\eta = (\omega_n^l / \Omega_f)$, Equation (82) can be written as

$$\begin{aligned} \Omega_f \left[\frac{d\xi_n}{d\tau'} - i\eta\xi_n \right] &= \frac{\varepsilon}{t_n} \left(\int_0^1 \overline{\Phi}_n^T (\mathbf{L}'_1 + \mathbf{L}'_2) dx \right) \xi_n + \frac{\varepsilon\Omega_f}{t_n} \left(\int_0^1 \overline{\Phi}_n^T \mathbf{L}'_3 dx \right) \frac{d\xi_n}{d\tau'} \\ &+ \frac{\varepsilon}{t_n} \left(\int_0^1 \overline{\Phi}_n^T (\overline{\mathbf{L}}'_1 + \overline{\mathbf{L}}'_2) dx \right) \overline{\xi}_n + \frac{\varepsilon\Omega_f}{t_n} \left(\int_0^1 \overline{\Phi}_n^T \overline{\mathbf{L}}'_3 dx \right) \frac{d\overline{\xi}_n}{d\tau'}, \end{aligned} \quad (83)$$

where

$$\mathbf{L}'_j = \{l_j(x, \tau'), 0\}^T, \quad j = 1, 2, 3, \dots$$

Using Equation (61), one can write

$$\eta = 1 + \varepsilon\eta_1 + \dots \quad (84)$$

Now, we assume ξ_n in the form of the following series

$$\xi_n = \xi_n^{(0)} + \varepsilon\xi_n^{(1)} + \dots \quad (85)$$

Substituting Equations (84) and (85) into Equation (83) and equating the coefficients of the like powers of ε from both sides, we get:

$$\varepsilon^0 : \frac{d\xi_n^{(0)}}{d\tau'} - i\xi_n^{(0)} = 0. \quad (86)$$

$$\begin{aligned} \varepsilon^1 : \frac{d\xi_n^{(1)}}{d\tau'} - i\xi_n^{(1)} &= i\eta_1\xi_n^{(0)} + \frac{1}{\omega_n^l t_n} \left(\int_0^1 \overline{\Phi}_n^T (\mathbf{L}'_1 + \mathbf{L}'_2) dx \right) \xi_n \\ &+ \frac{1}{t_n} \left(\int_0^1 \overline{\Phi}_n^T \mathbf{L}'_3 dx \right) \frac{d\xi_n^{(0)}}{d\tau'} \\ &+ \frac{1}{\omega_n^l t_n} \left(\int_0^1 \overline{\Phi}_n^T (\overline{\mathbf{L}}'_1 + \overline{\mathbf{L}}'_2) dx \right) \overline{\xi}_n^{(0)} \\ &+ \frac{1}{t_n} \left(\int_0^1 \overline{\Phi}_n^T \overline{\mathbf{L}}'_3 dx \right) \frac{d\overline{\xi}_n^{(0)}}{d\tau'}. \end{aligned} \quad (87)$$

First we substitute the following solution of Equation (86)

$$\xi_n^{(0)} = be^{i\tau'}$$

into Equation (87). Then, to avoid secular terms in $\xi_n^{(1)}$, the following condition must hold:

$$(\eta_1 - \Gamma_1)b - \Gamma_2\overline{b} + \left(\frac{e'_0}{\omega_n^l} \right) Ge^{-2i\theta_n}\overline{b} + i \left(\frac{\mu'}{\omega_n^l} \right) b = 0, \quad (88)$$

where

$$\Gamma_1 = \frac{k}{4} \tilde{a}_n^2 \left[2 \left(\int_0^1 \left(\frac{d\phi_n}{dx} \right)^2 dx \right) \left(\int_0^1 \frac{d^2 \bar{\phi}_n}{dx^2} \bar{\phi}_n dx \right) + 4 \left(\int_0^1 \frac{d\bar{\phi}_n}{dx} \frac{d\phi_n}{dx} dx \right) \left(\int_0^1 \frac{d^2 \phi_n}{dx^2} \bar{\phi}_n dx \right) \right] / t_n$$

and

$$\Gamma_2 = \frac{k}{4} \tilde{a}_n^2 \left[\left(\int_0^1 \left(\frac{d\phi_n}{dx} \right)^2 dx \right) \left(\int_0^1 \frac{d^2 \bar{\phi}_n}{dx^2} \bar{\phi}_n dx \right) + 2 \left(\int_0^1 \frac{d\bar{\phi}_n}{dx} \frac{d\phi_n}{dx} dx \right) \left(\int_0^1 \frac{d^2 \phi_n}{dx^2} \bar{\phi}_n dx \right) \right] / t_n.$$

For the existence of a non-trivial solution of $b (= b_x + ib_y)$ from Equation (88) one finally obtains (after some algebraic manipulations):

$$\eta_1 = \Gamma_1 \pm \left[\Gamma_2^2 - 2\Gamma_2 \left(\frac{e'_0}{\omega_n^l} \right) A_1 + \left(\frac{e'_0}{\omega_n^l} \right)^2 \left((G^R)^2 + (G^I)^2 \right) - \left(\frac{\mu'}{\omega_n^l} \right)^2 \right]^{1/2} \quad (89)$$

with $A_1 = G^R \cos 2\theta_n + G^I \sin 2\theta_n$. In the $\tilde{a}_n - \Omega_f$ plane, Equation (89) implies two curves

$$\Omega_{fs}^{(j)} = \omega_n^l (1 - \varepsilon \eta_1^{(j)}), \quad j = 1, 2,$$

where $\eta_1^{(j)}$ corresponds to either of the values of η_1 from Equation (89) and $\Omega_{fs}^{(j)}$ denotes the associated stability boundary.

For a fixed value of \tilde{a}_n and θ_n , $\Omega_{fs}^{(j)}$'s are calculated first ($\Omega_{fs}^{(1)} < \Omega_{fs}^{(2)}$, say) and then checked with the forcing frequency Ω_f . The amplitude is said to be unstable if

$$\Omega_{fs}^{(1)} < \Omega_f < \Omega_{fs}^{(2)} \quad (90)$$

and stable otherwise.

It is to be noted from Equation (89) that for some values of the parameters, η_1 does not exist. This implies a stable condition under such circumstances.

References

1. Wickert, J. A. and Mote Jr., C. D., 'Current research on the vibration and stability of axially moving materials', *Shock and Vibration Digest* **20**(5), 1988, 3–13.
2. Naguleswaran, S. and Williams, C. J. H., 'Lateral vibrations of band-saw blades pulley belts and like', *International Journal of Mechanical Science* **10**, 1968, 239–250.
3. Asokanthan, S. F. and Ariaratnam, S. T., 'Flexural instabilities in axially moving bands', *ASME Journal of Vibration and Acoustics* **116**, 1994, 275–279.
4. Pakdemirli, M., Ulsoy, A. G., and Ceranoglu, A., 'Transverse vibration of an axially accelerating string', *Journal of Sound and Vibration* **169**(2), 1994, 179–196.

5. Nayfeh, A. H. and Mook, D. T., *Nonlinear Oscillations*, Wiley, New York, 1979.
6. Mockenstrum, E. M., Perkins, N. C., and Ulsoy, A. G., 'Stability and limit cycles of parametrically excited, axially moving strings', *ASME Journal of Vibration and Acoustics* **118**, 1996, 346–350.
7. Troger, H. and Hsu, C. S., 'Response of a nonlinear system under combined parametric and forcing excitation', *ASME Journal of Applied Mechanics* **44**, 1977, 179–181.
8. Zavodney, L. D., Nayfeh, A. H., and Sanchez, N. E., 'The response of a single-degree-of-freedom system with quadratic and cubic non-linearities to a principal parametric resonance', *Journal of Sound and Vibration* **129**(3), 1989, 417–422.
9. Chakraborty, G., Mallik, A. K., and Hatwal, H., 'Normal modes and near-resonance response of beams with non-linear effects', *Journal of Sound and Vibration* **210**(1), 1998, 19–36.
10. Chakraborty, G., Mallik, A. K., and Hatwal, H., 'Non-linear vibration of a traveling beam', *International Journal of Non-Linear Mechanics* (in press).
11. Thurman, A. L. and Mote Jr., C. D., 'Free periodic non-linear oscillations of an axially moving strip', *ASME Journal of Applied Mechanics* **36**, 1969, 83–89.
12. Mote Jr., C. D., 'A study of band saw vibrations', *Journal of Franklin Institute* **279**, 1965, 430–444.
13. Wang, K. W. and Mote Jr., C. D., 'Vibration coupling analysis of band/wheel mechanical systems', *Journal of Sound and Vibration* **109**, 1986, 237–258.
14. Al-Jawi, A. A. N., Pierre, C., and Ulsoy, A. G., 'Vibration localization in dual span axially moving beams. Part I: Formulation and results; Part II: Perturbation analysis', *Journal of Sound and Vibration* **179**(2), 1995, 289–312.
15. Hwang, S.-J. and Perkins, N. C., 'High speed stability of coupled band/wheel systems: theory and experiment', *Journal of Sound and Vibration* **169**, 1994, 459–483.
16. Hwang, S.-J. and Perkins, N. C., 'Super-critical stability of an axially moving beam. Part I: Model and equilibrium analysis; Part II: Vibration and stability analysis', *Journal of Sound and Vibration* **154**, 1992, 381–409.
17. Wang, K. W., 'Dynamic stability analysis of high speed axially moving bands with end curvature', *ASME Journal of Vibration and Acoustics* **113**, 1991, 62–68.
18. Wickert, J. A. and Mote Jr., C. D., 'Classical vibration analysis of axially moving continua', *ASME Journal of Applied Mechanics* **57**, 1990, 738–744.